Supporting Information

Co-precipitation synthesis control for sodium ion adsorption capacity and cycle life of copper hexacyanoferrate electrodes in battery electrode deionization

Le Shi [a], Xiangyu Bi [a], Evan Newcomer [a], Derek M. Hall [b], Christopher A. Gorski [a], Ahmed Galal [c], Bruce E. Logan [a,*]

a. Department of Civil and Environmental Engineering, The Pennsylvania State University, University Park, PA 16802, USA
b. Department of Energy and Mineral Engineering, The Pennsylvania State University, University Park, PA 16802, USA
c. Chemistry Department, Faculty of Science, Cairo University, 12613, Giza, Egypt

*Corresponding author. Email: blogan@psu.edu; Tel.: +1-814-863-7908

Number of pages: 10

Number of figures: 6

Number of tables: 5

Table S1. ICP-OES results of CuHCF powders prepared under different conditions.

Sample	Molar concentration / mmol g^{-1}				Normalized formula on Fe unit				stoichiometry
	K	Na	Cu	Fe	K	Na	Cu	Fe	
1	0.125	0.002	3.678	2.630	0.05	0	1.4	1	$K_{0.05}Cu_{1.4}[Fe(CN)_6]$
2a	0.219	1.994	3.112	1.422	0.15	1.4	2.19	1	$Na_{1.4}K_{0.15}Cu_{2.19}[Fe(CN)_6]$
2b	0.726	0.771	2.939	2.006	0.36	0.39	1.47	1	$Na_{0.39}K_{0.36}Cu_{1.47}[Fe(CN)_6]$
2c	1.723	5.136	1.765	1.030	1.67	4.98	1.71	1	$Na_{4.98}K_{1.67}Cu_{1.71}[Fe(CN)_6]$
3a	2.291	0.699	3.164	2.176	1.05	0.32	1.45	1	$Na_{0.32}K_{1.05}Cu_{1.45}[Fe(CN)_6]$
3b	2.232	0.364	2.933	2.225	1.00	0.16	1.32	1	$Na_{0.16}K_{1.00}Cu_{1.32}[Fe(CN)_6]$
4a	2.402	0.551	2.987	2.329	1.03	0.24	1.28	1	$Na_{0.24}K_{1.03}Cu_{1.728}[Fe(CN)]$
4b	2.569	0.377	2.928	2.378	1.08	0.16	1.23	1	$Na_{0.16}K_{1.08}Cu_{1.23}[Fe(CN)_6]$

By normalizing the molar concentration of each element to Fe unit, the stoichiometry $Na_mK_nCu_x[Fe(CN)_6]$ can be determined and summarized in Table S1. However, C or N element could not be detected through ICP as it could only analyze metal elements, therefore we assume that 6 CN^- were coordinated with 1 Fe.

The crystal sizes of each sample (summarized in Table S2) are calculated using the Scherrer formula:

$$L = \frac{K\lambda}{\beta cos\theta}$$

where *L* is the size of the ordered (crystalline) domains, *K* is a dimensionless shape factor, with a typical value of 0.94 was used in this work, λ is the wavelength of the X-ray radiation (1.5406 Å), β is the peak width at the half-maximum intensity, after subtracting the instrumental line broadening, θ is the Bragg diffraction angle.

Table S2. XRD crystalline size calculation based on (200) peak and unit cell parameter of each CuHCF pristine powder sample.

Sample	Peak position	Peak width (FWHM)	Crystallite size (nm)	Unit cell (Å)
1	17.582	0.171	78.962	10.102
2a	17.638	0.198	62.694	10.032
2b	17.648	0.241	47.527	10.038
2c	17.701	0.196	63.593	10.028
3a	17.672	0.312	33.903	10.020
3b	17.668	0.339	30.626	10.025
4a	17.669	0.462	21.138	10.027
4b	17.628	0.633	14.776	10.026

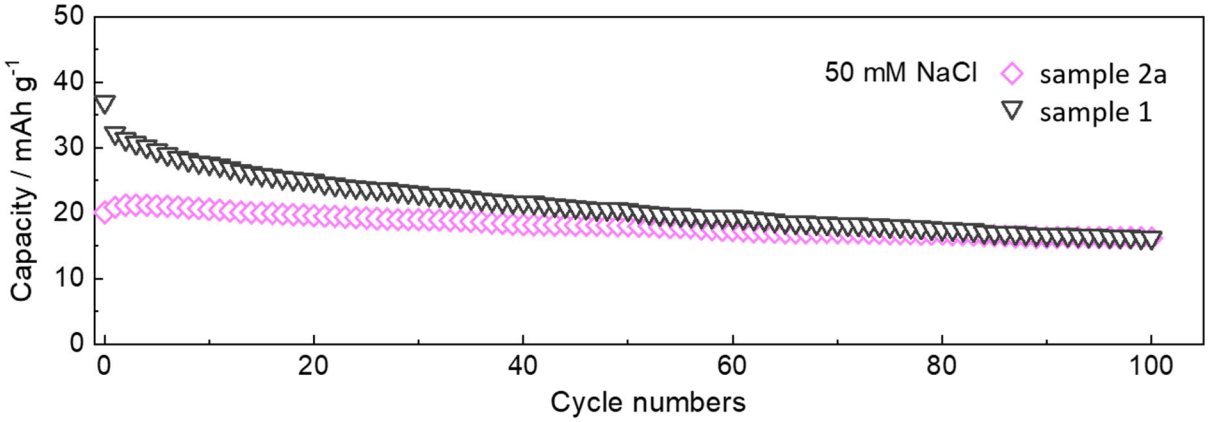

Figure S1. Cycling performance of CuHCF-based electrodes with powder sample 1 and 2a over 100 cycles in the BDI flow cell with 50 mM NaCl feed solution. A constant current of 7 mA/30mg was applied in the voltage window of ± 0.6 V with a flow rate of 0.5 mL/min.

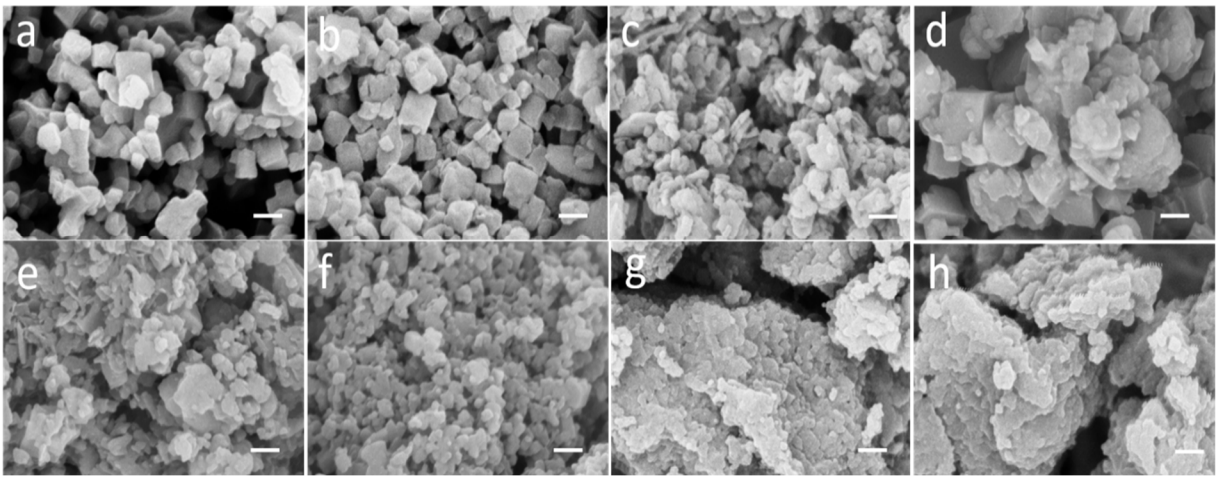

Figure S2. Scanning electron microscopy (SEM) images of CuHCF pristine powder (sample 1-4). The scale bar is 100 nm.

Table S3. Weight loss % of CuHCF pristine powder samples from thermogravimetric analysis (TGA). The TGA test was carried out under N_2 atmosphere from room temperature to 600 °C at a ramp rate of 10 °C/min.

Sample	Absorbed	Zeolitic	Coordinated	Thermal
1	11.2	12.3	3.9	5.2
2a	8.7	6.6	13.6	5.1
2b	8.2	8.6	13.8	7.9
2c	2.8	8.1	6.1	2.4
3a	6.2	8.2	-	5.5
3b	7.5	6.6	-	6.9
4a	6.2	5.3	-	5.2
4b	5.8	4.7		5.2

Table S4. The redox potential (E_{half}/V) and the potential difference between the oxidation and reduction reactions (ΔE/V) of each CuHCF-based electrode based on peak O1 and R1. The CV data were measured at 1 mV/s in the potential window of -0.3 to 1.1 V (vs Ag/Ag/Cl) in 1 M NaCl solution.

sample	E_{half}/V	ΔE/V
1	0.629	0.221
2a	0.711	0.114
2b	0.641	0.171
2c	0.667	0.093
3a	0.627	0.208
3b	0.611	0.208
4a	0.622	0.205
4b	0.621	0.222

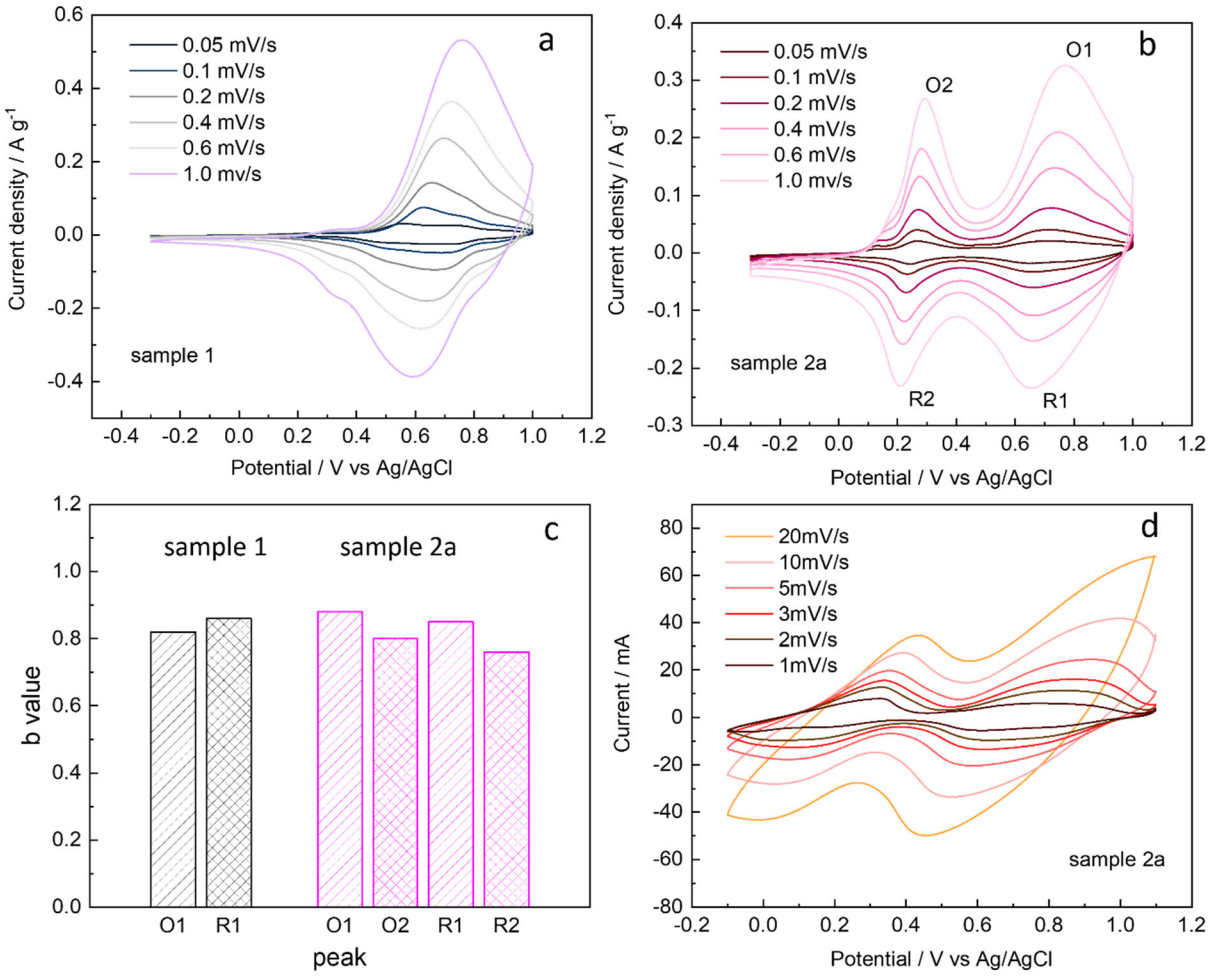

Figure S3. Cyclic voltammetry (CV) of CuHCF-based electrode sample 1 (a) and 2a (b) under series of scan rates from 0.05 to 1.0 mV/s in 1M NaCl solution. O1/R1 peaks correspond to the oxidation and reduction of the Fe^{III}/Fe^{II} redox couple, while O2/R2 peaks correspond to the Cu^{II}/Cu^{I} redox couple. The b values derived from the CV curves of each peak current (c). CV of sample 2a under series of scan rates from 1.0 to 20 mV/s in 1M NaCl solution (d).

The voltammetric response in Figure S2 follows a power-law relationship of measured current with the scan rate according to:[1]

$$i = av^b$$

where i is the measured peak current (A/g), v is the scan rates (mv/s), both a and b are adjustable parameters.

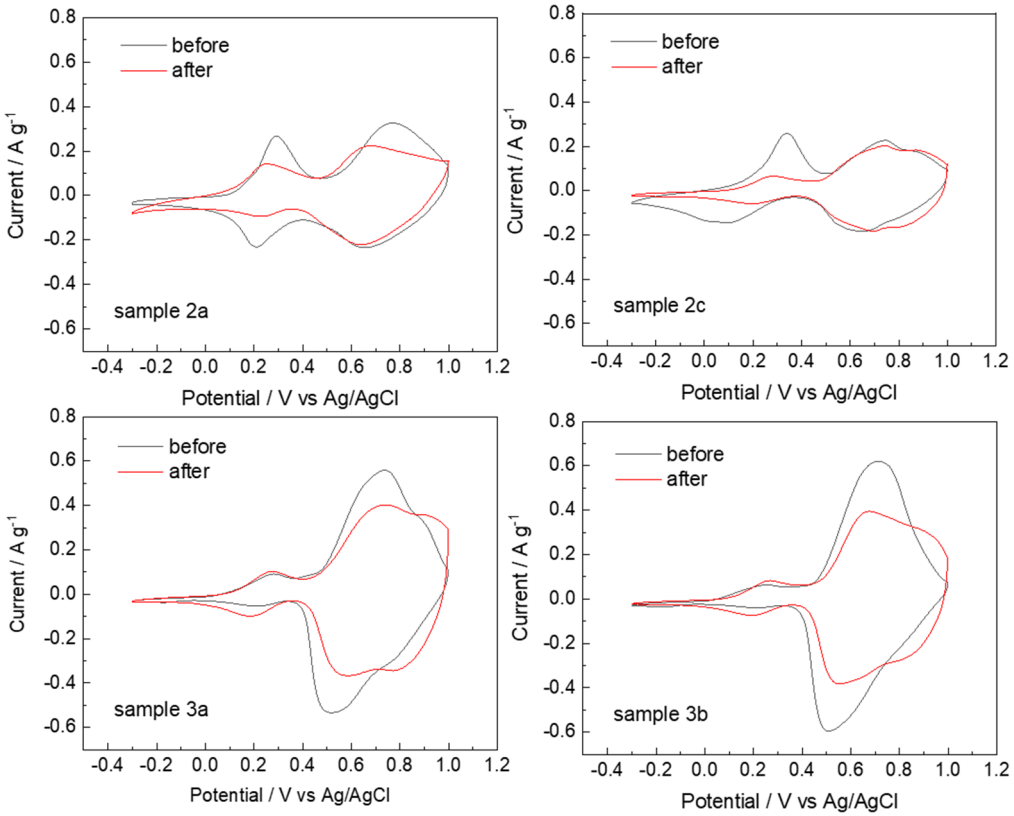

Figure S4. Cyclic voltammetry (CV) of CuHCF-based electrodes with sample 2a, 2c, 3a and 3b before and after BDI cycling for 100 times (with scan rate of 1 mV/s in the potential window of -0.3 to 1.0 V in 1M NaCl solution).

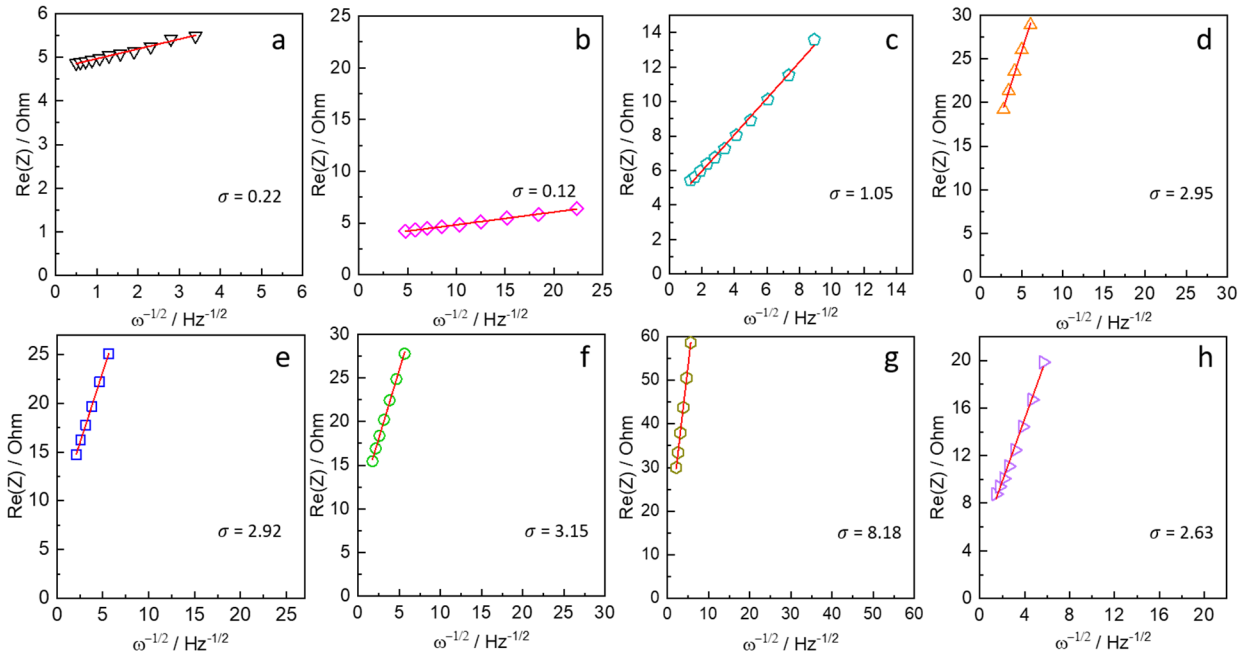

Figure S5. The plots of impedance as a function of the inverse square root of angular frequency in the Warburg region in Nyquist plots in **Figure 5**.

The Warburg impedance associated with the diffusion of ions is given by the following equation[2]:

$$Z_W = \sigma\omega^{-\frac{1}{2}}(1-j)$$

where σ is the Warburg coefficient and ω are the Warburg coefficient and angular frequency of the probing signal.

Calculation of Na^+ apparent diffusion coefficients through EIS results

The diffusion coefficient value (D, cm^2s^{-1}) can be calculated from the following equation[3]:

$$D = \frac{R^2T^2}{2A^2n^4F^4C^2\sigma^2}$$

where σ is the Warburg coefficient associated with Z_{Re}, R is the gas constant (8.314 J mol^{-1} K^{-1}), T is the absolute temperature (K), A is the surface area of electrode (cm^2), n is the number of electrons per molecule during oxidization, F is the Faraday's constant (96485.3329 C/mol), C is the Na^+ concentration. The Warburg coefficient σ can be obtained from the slope of the linear fitting Z_{Re} to square root of the corresponding angular frequency ω in the low frequency region, while R_e and R_{ct} kinetics parameters are independent of frequency. Therefore, the Warburg coefficient σ is obtained:

$$Z_{Re} = R_e + R_{ct} + \sigma\omega^{-1/2}$$

Table S5. The Warburg coefficient ($\sigma, \Omega/\sqrt{s}$), and apparent Na^+ diffusion coefficient (D, cm^2/s) of each sample obtained from Nyquist plots.

sample	$\sigma(\Omega/\sqrt{s})$	D (cm^2/s)
1	0.22	1.45×10^{-8}
2a	0.12	4.78×10^{-8}
2b	1.05	6.56×10^{-10}
2c	2.95	8.32×10^{-11}
3a	2.92	8.49×10^{-11}
3b	3.15	7.30×10^{-11}
4a	8.18	1.08×10^{-11}
4b	2.63	1.05×10^{-10}

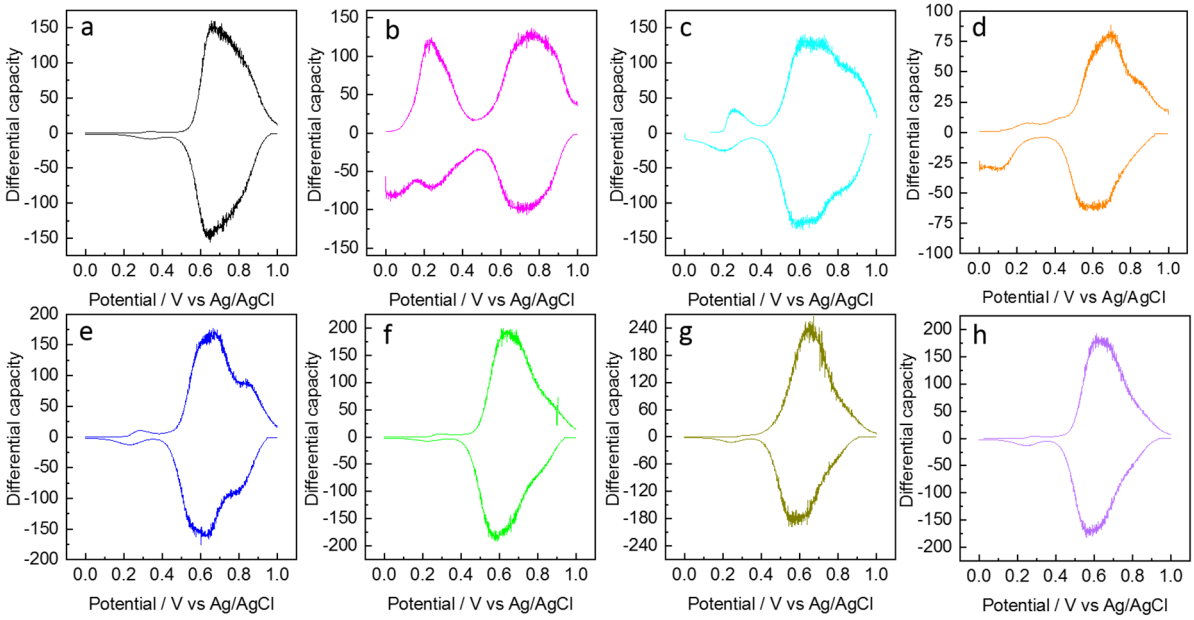

Figure S6. Differential capacity curves for galvanostatic charge and discharge curves in **Figure 6**.

References

(1) Wang, J.; Polleux, J.; Lim, J.; Dunn, B., Pseudocapacitive contributions to electrochemical energy storage in TiO_2 (anatase) nanoparticles. *J. Phys. Chem. C* **2007,** *111*, (40), 14925-14931.
(2) Janek, R. P.; Fawcett, W. R.; Ulman, A., Impedance spectroscopy of self-assembled monolayers on au(111): Sodium ferrocyanide charge transfer at modified electrodes. *Langmuir* **1998,** *14*, (11), 3011-3018.
(3) Ren, W.; Qin, M.; Zhu, Z.; Yan, M.; Li, Q.; Zhang, L.; Liu, D.; Mai, L., Activation of sodium storage sites in prussian blue analogues via surface etching. *Nano Lett.* **2017,** *17*, (8), 4713-4718.